

Numerical Simulation of Welding Influence on Tensile Strength and Residual Stress of AISI 304 Butt Joints

Open
Access

Adel Mahmoud Bash^{1,*}

¹ Department of Mechanical Engineering, College of Engineering, University of Tikrit, Tikrit, Iraq

ARTICLE INFO

Article history:

Received 11 August 2019

Received in revised form 12 September 2019

Accepted 1 October 2019

Available online 15 December 2019

ABSTRACT

Fusion welding is a metallurgical fusion process in which parts assembled by heating the connecting edge above the melting temperature and then compacting it. The present study was designed to determine the effect of TIG welding on the thermo-mechanical performance of AISI 304 butt joints. The aim can be achieved by employing three-dimensional analysis with non-linear thermo-mechanical simulations for AISI 304 stainless steel using finite element analysis. Moreover, the failure mode of butt joints under tensile stress test has been obtained numerically using finite element analysis. This study has shown that when the welding current increases, the heat input increased and the fusion zone area is decreased. The increase in welding current (increased heat input) leads to a reduction in the cooling rate and an increase in the grain size of the weld metal and the region affected by heat (heat affected zone). An increase in welding current increases the width of the region affected by heat and increases the volume fraction and decreases microhardness. The results showed that the longitudinal residual stress distribution is uniform along the weld line with similar pattern with transversal residual stress. Therefore, due to increase cooling rate, the microhardness has a maximum value at the boundary between the fusion zone and heat-affected zone. Nevertheless, it turned out that all coupons tested for butt joints fractured in the heat-affected zone (HAZ).

Keywords:

Tungsten Inert Gas (TIG) welding;
residual stresses; transient temperature;
tensile test; numerical simulation

Copyright © 2019 PENERBIT AKADEMIA BARU - All rights reserved

1. Introduction

Producing parts as a whole is, at some point, impossible because that part can consist of so many complicated shapes. Therefore, the topic of butt joint welding is one of the most active areas of metal joining technique research today. There is a consensus among social scientists that there are several categories of welding imperfections to produce fusion zones and heat-affected zones such as microstructure imperfections infusion and heat zones, hot and cold cracks in welding, deformation due to welding and residual stresses. All these imperfections are made during or after welding. Therefore, the investigation of heat transfer and heat input in welding is very imperative for

* Corresponding author.

E-mail address: adelbash@tu.edu.iq (Adel Mahmoud Bash)

identifying this defect. Fusion welding is a metallurgical fusion process in which parts assembled by heating the connecting edge above the melting temperature and then compacting it [1-3]. The numerical simulation of welding process can be considered an effective method to predicts the deformation and stresses of the welding, due to its advantage in reducing the time consumption to obtain the required analysis and reducing the scoop of experimental tests and speed up the process of the design optimization [4-6].

A numerical study has been established for the two-dimensional quasi-stationary model using finite element method for studying the phenomenon of heat transfer and fluid flow that arises in constant travel speeds, the keyhole plasma arc utilized to weld the metal plates [7]. The results displayed that the applied method can simulate the welding pool shape as a welding variables function. Moreover, fusion zones width and heat affected zone are increased due to welding speed decreases, meanwhile, the required power for the welding process increases with the increasing speed of welding.

The welding simulation of the tee and butt joints utilizing finite element method for the quasi-steady state analysis has been done by [8]. Where aluminium alloy 2519-T87 adopted as the base metal and alloy 2319 is the filler material. The results show that good agreement of maximum longitudinal normal residual stress with 3.6% deviation compared with published data, whereas the maximum stress of fully transient analysis was 13% deviation. In a different study a numerical analysis of the robotic welding by spot Tungsten Inert Gas (TIG) welding process using a software environment based on the finite element method has been achieved [9], the model adopted is applied to trajectory planning and speed control of the welding robot to achieve better quality welds in an automated system.

In a different study, Jiang *et al.*, [10] perform 3D finite element (FE) analysis using the double distribution of Goldak ellipsoidal heat source. The fields of residual stress and temperature in welds repair stainless steel plates have been considered in their study. The results detected that the length of the repair had effects on transverse stress, longitudinal stress and yield strength on welds and heat-affected zone. Chen C. *et al.*, [11] carried out a numerical study of the effect of the welding process on the stress-strain relation that represents by the tensile strength of high strength steel butt joints steel butt joint. The results showed that the increase in butt joint thickness leads to a decrease in joint strength under direct tensile test; this can be achieved only if the passing heat is maintained constant.

The residual stresses can be simulated numerically by modelling virtual processes in finite element models. Several solvers such as ANSYS and Abaqus based on finite element method have the capability to simulate residual stresses utilizing user subroutines [12]. In another numerical study, a mapping procedure utilizing predetermined stress results by the finite element analysis has been presented to evaluate the field of butt-welded plate residual stress with limited measurement results [13, 14].

However, the method of stress function and the reverse problem has been considered particularly useful if the distribution of eigenstrain or residual stress can be estimated precisely [15]. Nevertheless, stress values charted in the author study may case non-uniform solutions in the finite element solver because of imbalances presented with pressure in small areas. The characteristic of residual stress properties is that in the absence of external loads the stress must be balanced. Usually, in the most experiment measuring residual stress, areas with low residual stresses under areas with high residual stress are arranged. As a result, measurement data is usually incomplete. Therefore, the use of this measurement data as an initial data in finite element model produces an unbalanced stress field. This state has been clearly described and explained the influence of partial measurements of residual stress on the assessment of the intensity factor of the stress [16, 17].

To intensely understand the fundamental mechanisms associated with the welding process and enhance the quality of (TIG) welding of AISI 304 sheets of steel, simulations and numerical modelling of residual stresses and transient temperatures are useful and indispensable. Therefore, the aim of this study is to numerically examine the effect of TIG welding on the thermo-mechanical performance of AISI 304 butt joints. The aim can be achieved by employing three-dimensional analysis with non-linear thermo-mechanical simulations for 304 stainless steel using finite element analysis. The parameters of present numerical determination are the current of welding of (130-150A) based on the speed of welding with 8mm plate thickness, as well as the material of heat sink, which is copper. Results for transient temperature, tensile tests and residual stress are compared with available experimental data to validate this simulation. The coupon direct tensile test is carried out to determine the impact of welding on the butt joint tensile behaviour. The simulation procedure for the prediction of joint strength is adopted and its accuracy is validated by comparing the finding of the modelling with the finding of the tensile test.

2. Finite Element Analysis

The finite element method is employed to examine the impact of TIG welding on temperature distribution and residual stress as well as the tensile test of AISL 304 butt joint. In the numerical procedure, the finite element method was applied using ANSYS [18] to analyse the thermomechanical performance of the welded coupon. Moreover, in order to obtain identical results to the results of [19], similar boundary conditions to the experimental conditions must be adopted. The heat conduction governing equation of anisotropic solid, homogenous deprived of generated heat in the (x, y, z) system can be stated as [3].

$$\frac{\partial}{\partial x} \left[K \frac{\partial T}{\partial x} \right] + \frac{\partial}{\partial y} \left[K \frac{\partial T}{\partial y} \right] + \frac{\partial}{\partial z} \left[K \frac{\partial T}{\partial z} \right] = \rho c \frac{\partial T}{\partial t} \quad (1)$$

where the samples of (K, T, ρ , c, and t) refer to the thermal conductivity, temperature, material density, specific heat, and time respectively [20]. The initial boundary conditions are considered as the initial temperature determined for Tungsten Inert Gas (TIG) welding which includes all specimen elements as explained in Eq. (2). However, the energy balance of heat supply and heat losses is employed to establish a second boundary condition on the work surface where T^∞ denotes to the ambient temperature.

$$T = T^\infty \text{ at time} = 0 \quad (2)$$

The specific heat flows acting over surface in the initial boundary condition, can be represented with two equal components which are the heat flux acting as a normal conduction to the specimen surface and given by (q_n), and (n) refer to the unit outward normal vector, and the supplied heat flux to the specimen surface form TIG welding as a heat source and given by (q_{sup}) as explained in the bellow mentioned Eq. (3).

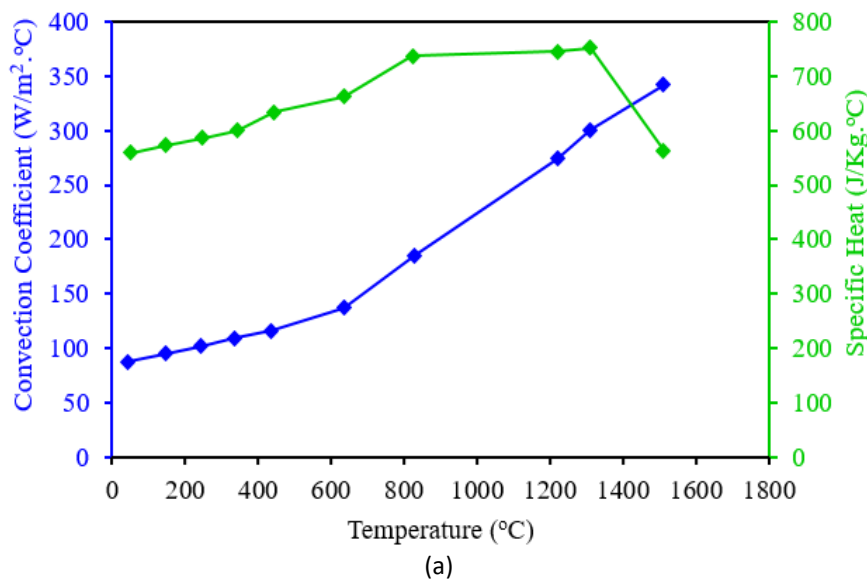
$$q_n = q_{sup} = \{q\}^T \{n\} \quad (3)$$

in the second boundary condition, the heat loss as a result of heat transfer convection over the surface has been calculated based on Newton's law as shown in Eq. (4) where (h) refers to convective heat transfer coefficient (W/m^2K).

$$Q_{conv} = h(T - T_{\infty}) \tag{4}$$

2.1 Numerical Analysis

The numerical simulation based on finite element analysis has been widely used in modelling of welding process and residual stress of welded joints. In the previous study, several finite element models assumed that the material properties of steel would deteriorate during the heating phase. The distribution of the residual stresses, transient temperature and tensile tests were studied using the Thermomechanical Finite Element Method for Tungsten Inert Gas (TIG) welding of austenitic steel AISI 304. The thermal and mechanical properties of AISI 304 steel [21] are shown in Figure 1 and Figure 2. The thermomechanical properties are used in finite element analysis with a three-dimensions model with respect temperature-dependent boundary condition of 25°C ambient temperature. In order to estimate the results, two stages were adopted by employing finite element analysis, first is the distribution of transient temperature of thermal analysis, second is the estimation of residual stresses and tensile test. Moreover, the temperature history has been used as input of thermal load and the impact of welding parameters such as TIG welding current on thermal history, distribution of temperature and residual stresses have been investigated. The dimension of the AISI 304 Steel sheet and cut out the block for tensile tests are presented in Figure 3.



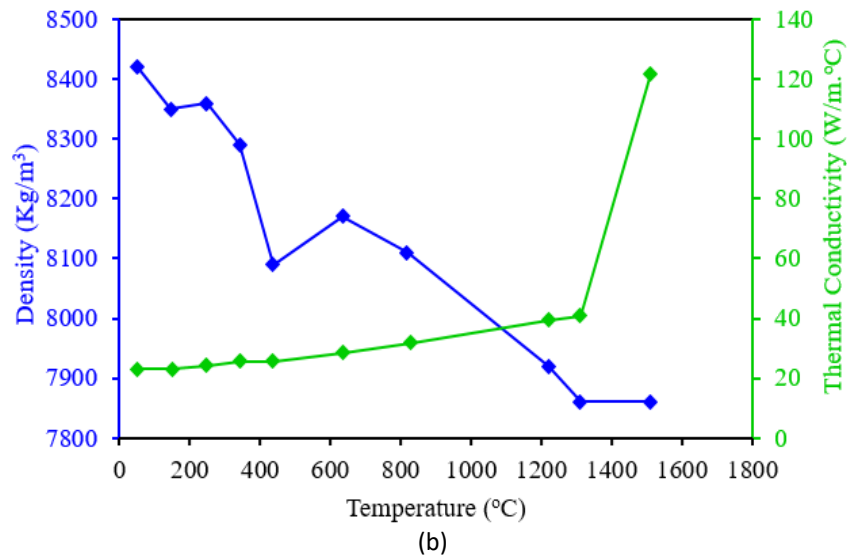


Fig. 1. Thermal properties of AISI 304 Steel sheet in (a) convection coefficient and specific heat and (b) density and thermal conductivity

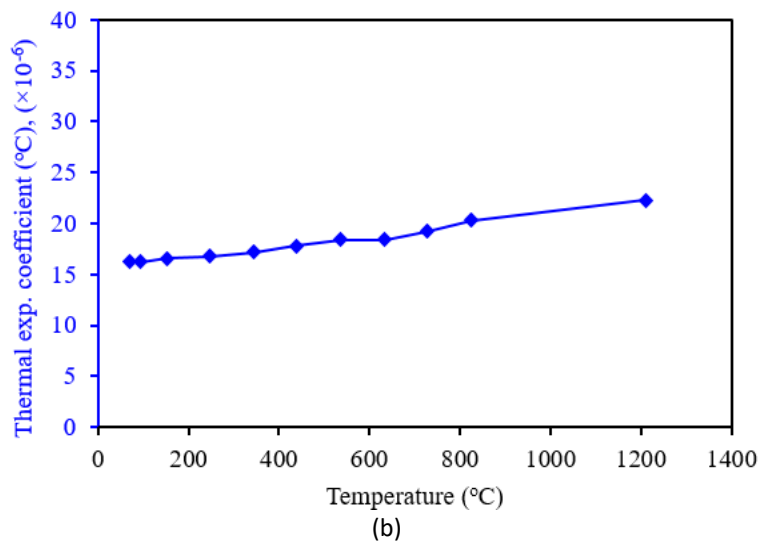
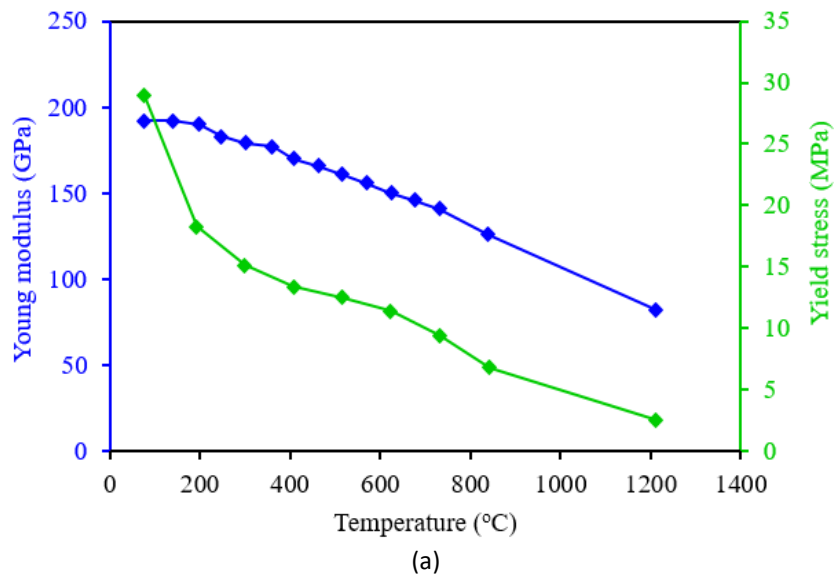


Fig. 2. Mechanical properties of AISI 304 Steel sheet; (a) Young modulus and Yield stress and (b) thermal expansion coefficient

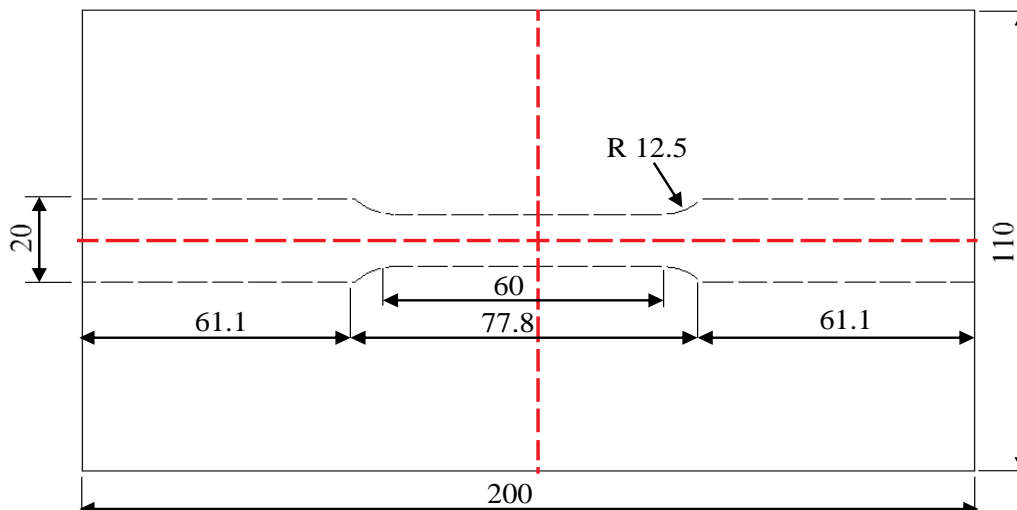


Fig. 3. The dimension of the AISI 304 Steel sheet and cut out the block for tensile tests

3. Results and Discussion

3.1 Verification of the Numerical Model

In order to validate the proposed model comparison between the current numerical model and the numerical results of [11] with the failure mode of coupon tensile test of butt joints in the direct tensile test have been carried out. A fine mesh sensitivity analysis was performed to estimate the best meshing parameters such as a number of elements and element size. The investigated plate is discretized utilizing shell elements with the integration of eight nodes, each element has six degrees of freedom on each node. Several different element sizes of 2.0, 1.5, 1.0 and 0.5 that represented as nodes number of 33105, 57684, 124603 and 191529 have been carried out to confirm that the estimated results are grid-independent.

It is illustrated in Figure 4 that increasing the element size does not change significantly the temperature and cooling time of the tested model of the composite plate. Therefore, the grid consisted of an element size of (1.0) which represented as nodes number of (124603) has been selected for the present study as illustrated in Figure 5. Moreover, for all the studied geometries the element size of 1.0 has been adopted for the current calculation. The existing case boundary conditions that represented the expressed plate support are determined by obstructive the nodes kinematic degrees of freedom that positioned on the plates at the top and bottom edges. The FEM model is achieved by implementing consistent tension load to the top edge of the plate. The direct tensile test has been employed to study the butt joint tensile behaviour of AISI 304 steel using finite element analysis. For analysis model of the direct tensile stress, because the finite mesh elements for coupons are implanted in mesh used to simulate welding, the history of nodal temperatures gained in a model of thermal analysis can be assigned directly to the mesh coupon nodes. Subsequently, of importing the data of temperature history, the tensile test is simulated as a quasi-static large strain and standard analysis of nonlinear material to estimate the mechanical behaviour of the butt joint specimen. The 8-node linear brick of C3D8 element is employed for test coupon modelling and the numerical model physical boundary conditions are estimated based on the experimental set [22]. The mesh of the numerical model with the tensile test coupon is illustrated as Figure 6.

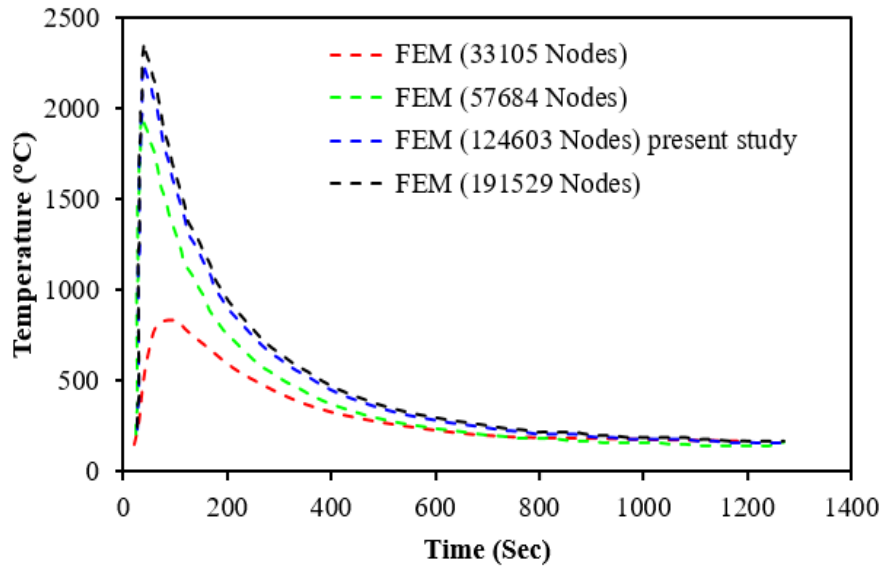


Fig. 4. Grid independent tests of the numerical model of AISI 304 Steel at welding current of (150 A)

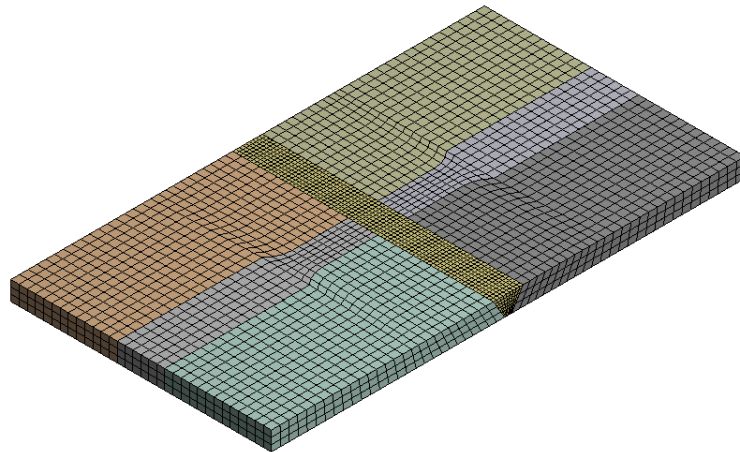


Fig. 5. The numerical model of AISI 304 Steel butt joint

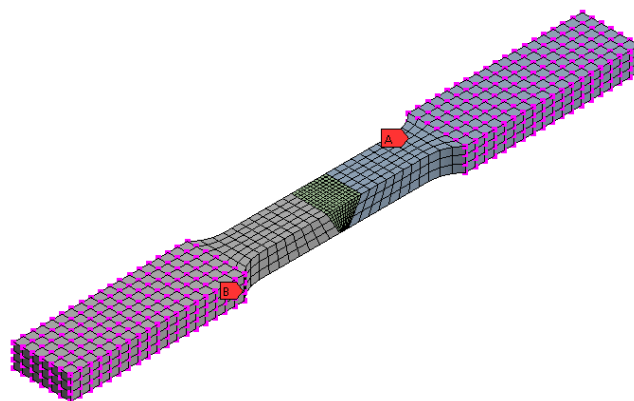


Fig. 6. Numerical model for tensile strength analysis

3.2 Temperature History

Effect of welding current on the temperature distribution has been investigated. Welding current is the most important factor that effecting on microhardness. The hardness drops with increasing the

welding current or heat input which increases the width of weld metal and heat affected zone [23]. Figure 7-9 show the computational temperature contours for the 8 mm plates thickness subjected to welding current (130, 140 and 150 A) respectively at the time (1, 20, 80, and 120 sec. from starting welding process). The temperature history at welded joint surface represented and the peak temperature indicated within the fusion zone was (1952°C, 1960°C and 1981°C). The same trend as in case one is repeated here with noting that the solidification process starts for (150A) faster than that for (130A). The temperature distribution using 150A provide higher heat transfer rate compared with the distribution of temperature using 140A and 130A. It can clearly show in Figure 10 the effect of welding current on the temperature distribution along with the time factor. Therefore, due to increase cooling rate, the microhardness has a maximum value at the boundary between the fusion zone and heat-affected zone. Increasing welding current (increase the heat input) leads to a reduction in cooling rate and an increasing the grain size of weld metal and heat affected zone. An increase welding current lead to increases the width of heat-affected zone and increases the volume fraction and decreases the microhardness.

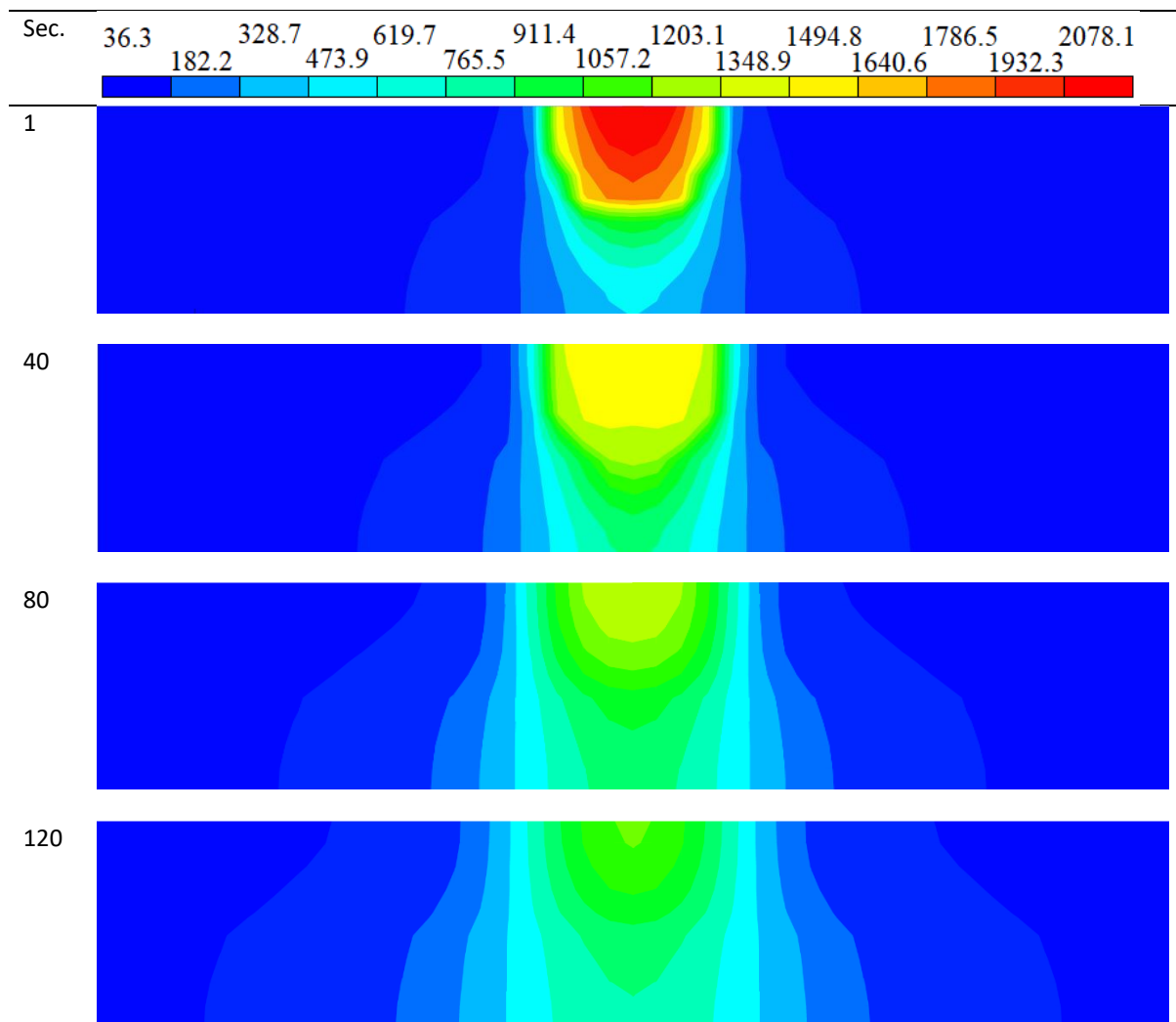


Fig. 7. The temperature distribution contours of welding current (130 A)

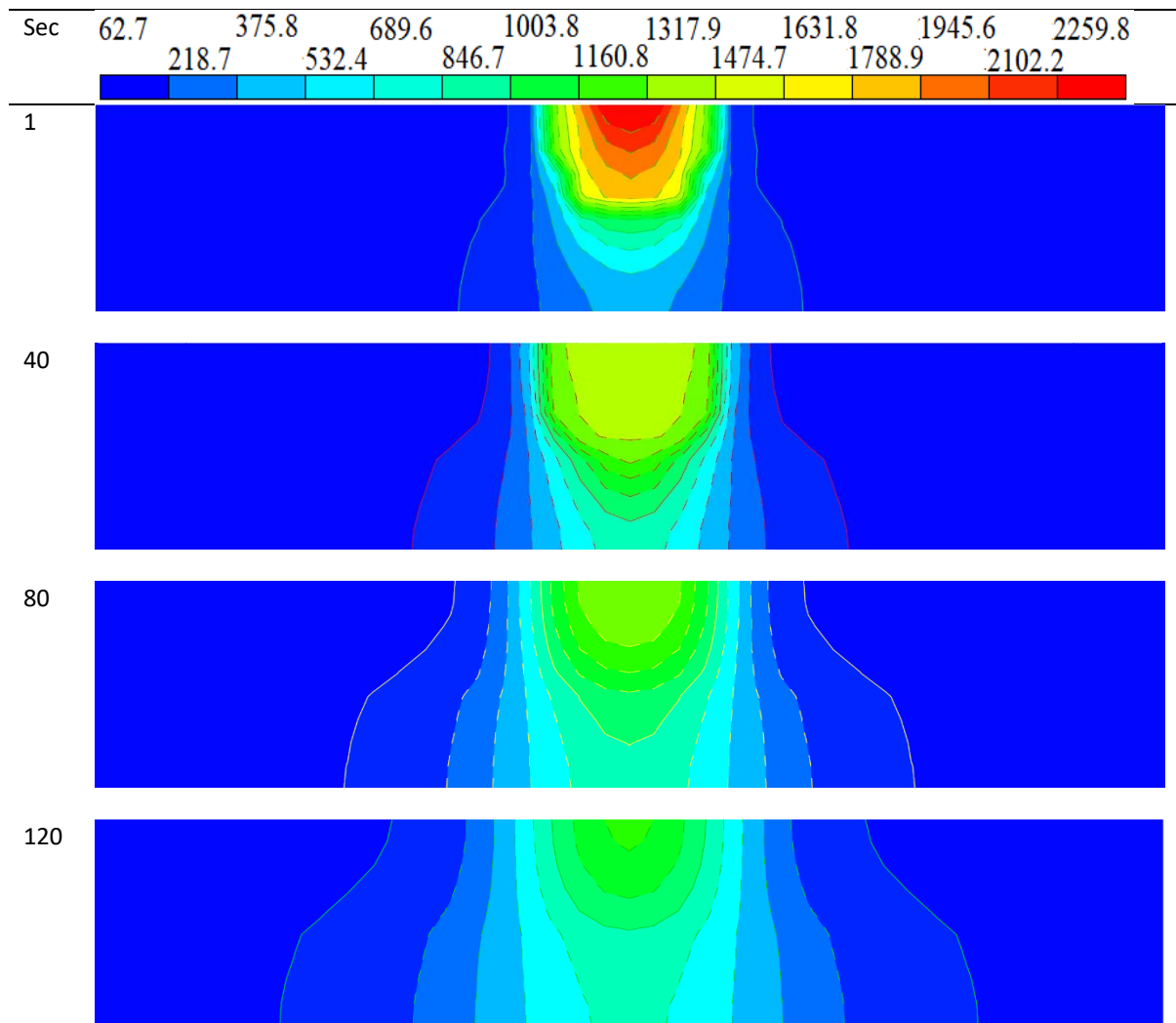


Fig. 8. The temperature distribution contours of welding current (140 A)

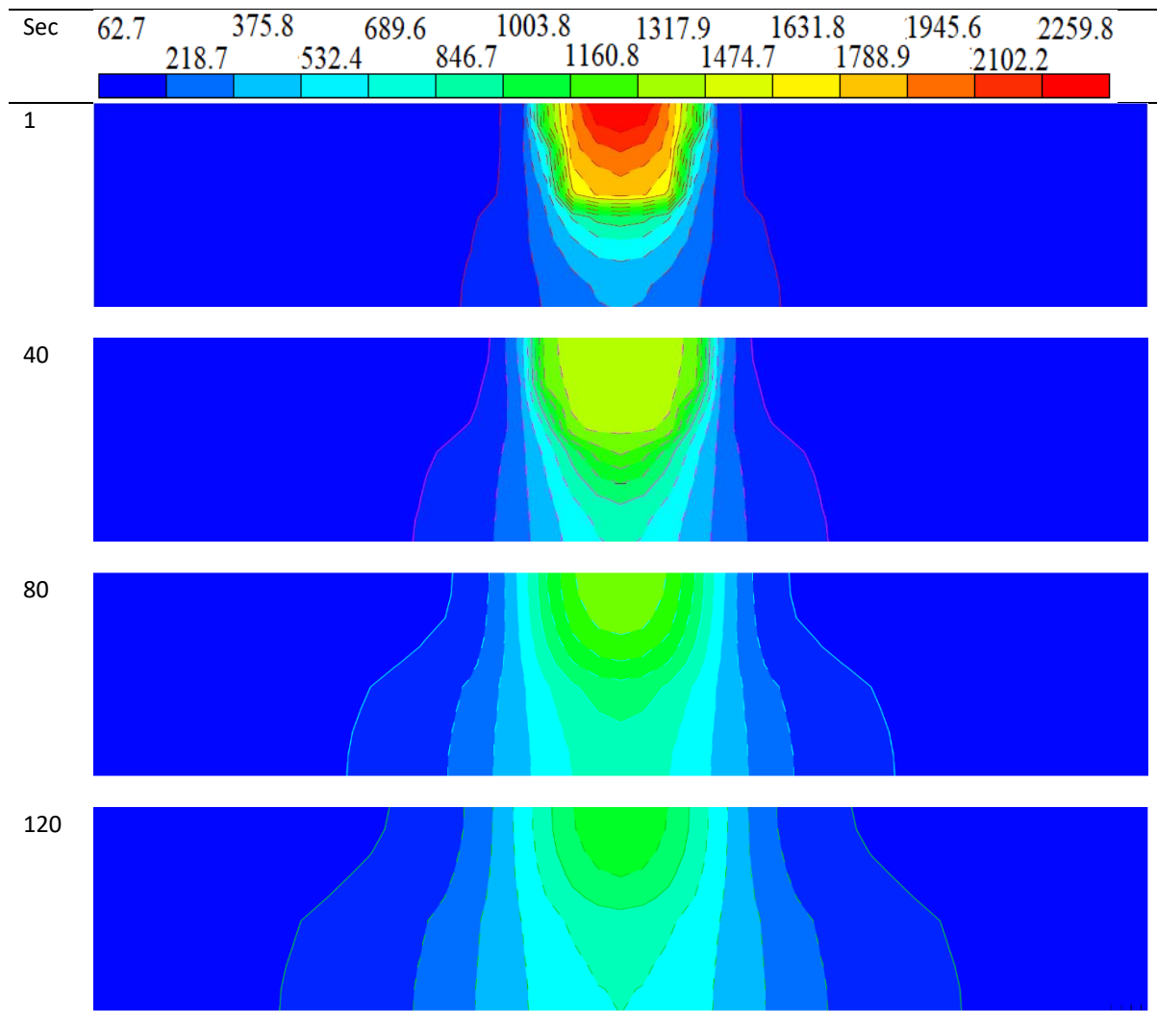


Fig. 9. The temperature distribution contours of welding current (150 A)

3.3 Residual Stress Results

The residual stresses can be simulated numerically by modelling simulated processes in finite element models. In this study, ANSYS solver based on the finite element method has the capability to simulate residual stresses utilizing user subroutines [12]. The stress distribution using the von mises method is represented as tensile strength and von mises stress pick value is similar to base metal yield strength. Moreover, Figure 11 and Figure 12 illustrate the distribution of residual stress by the von mises, transverse, and longitudinal residual stresses. The maximum magnitude of transverse residual stress is much lower than that of longitudinal residual stress. Additionally, Figure 10 and Figure 11 show that the pattern of stresses distribution on the top plate surface is approximately the same which is tensile in nature throughout the whole welded plate. Figure 12 shows that the distribution of von Mises, transversal and longitudinal residual stresses laterally the top welded line on the plate surface. The results showed that the longitudinal residual distributed stress is uniform laterally the line of welding with a similar pattern with transversal residual stress. However, at the starting and ending region of the weld line, the longitudinal and transversal residual stress have a compressive nature and its magnitude larger than longitudinal residual stress. Therefore, the relation among the input heat, welding temperature and material deformation is direct proportional relations [24].

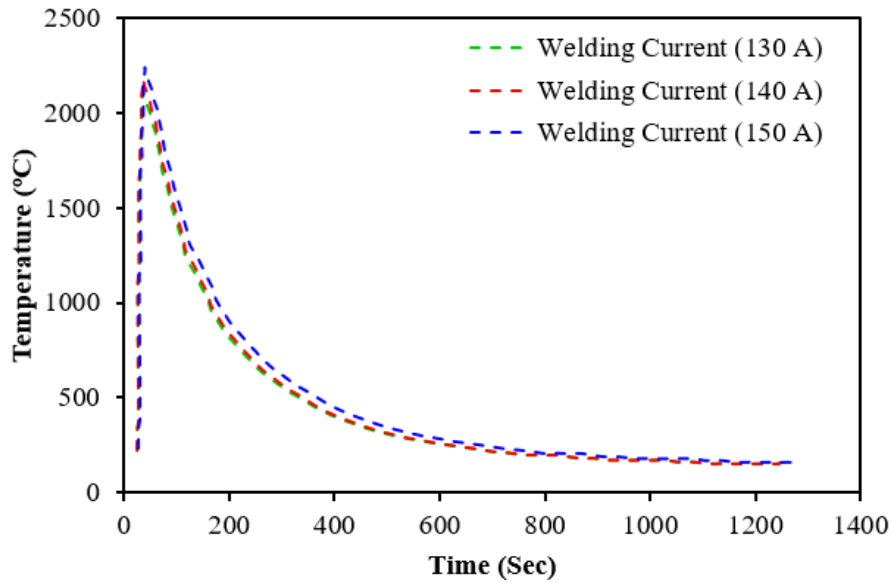


Fig. 10. The temperature history of welding current (130A, 140 A and 150A)

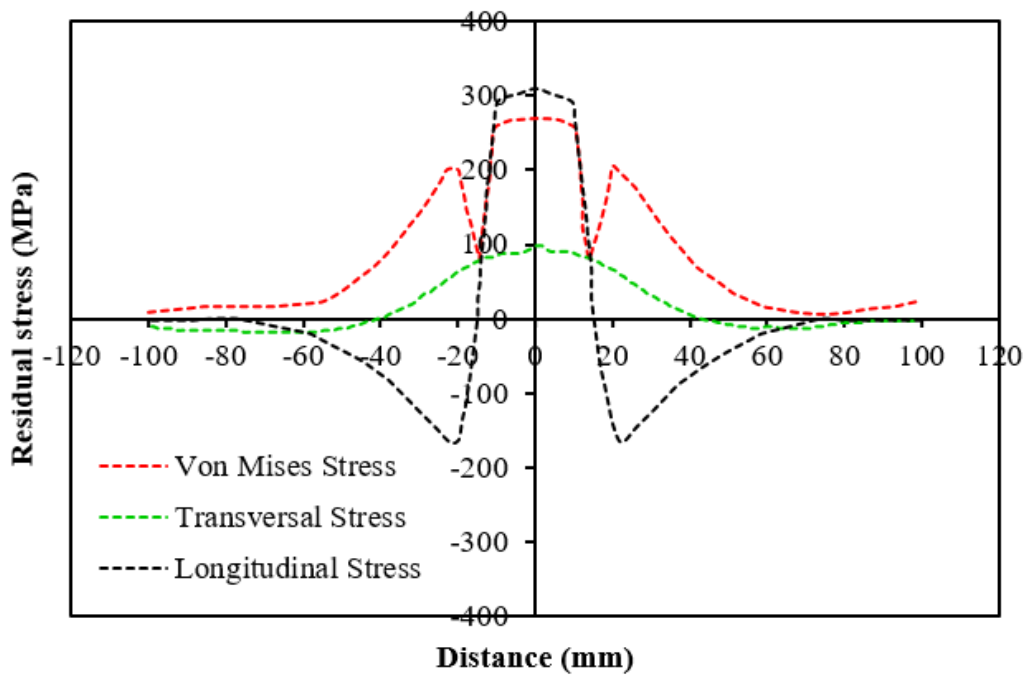


Fig. 11. Residual stress distributions normal to the weld line on the top surface based on Von Mises, transversal longitudinal methods

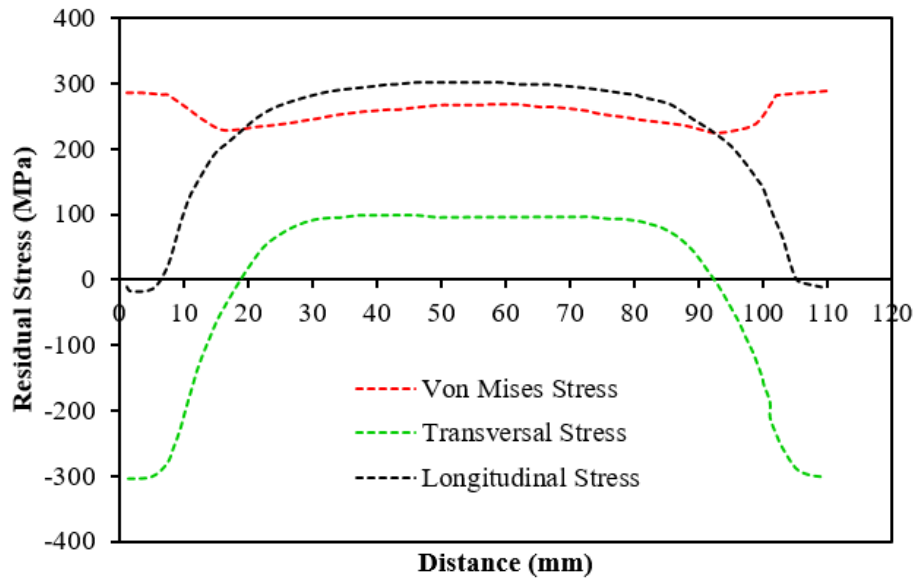
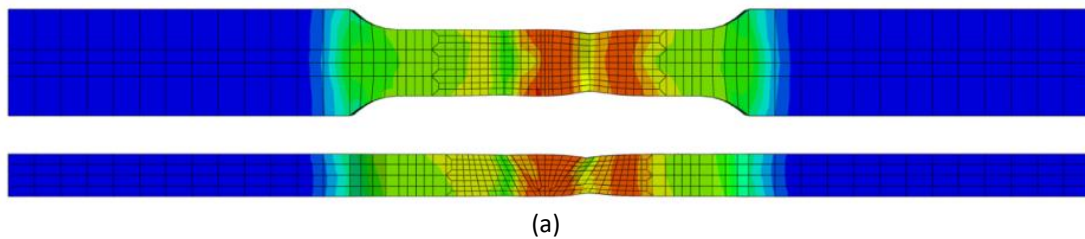
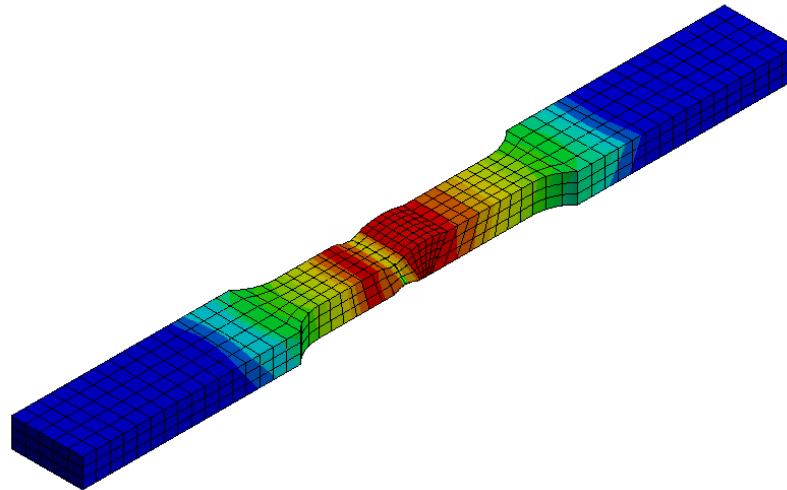


Fig. 12. Residual stress distributions along the weld line based on Von Mises, transversal Longitudinal, methods

3.4 Tensile Test Results

The failure mode of butt joints under tensile stress test has been obtained numerically using finite element analysis. A comparison between the current numerical model and the numerical results of [11] with the failure mode of coupon tensile test of butt joints in the direct tensile test have been illustrated in Figure 13. It's clearly shown in Figure 13 the finite element model displayed that the coupon of AISI 304 was failed at heat affected zone region by necking and fracture. Nevertheless, it turned out that all coupons tested for butt joints fractured in the heat affect zone (HAZ). Moreover, the failure mode with the stress-strain curves has been illustrated in Figure 14 for a wide range of temperature, the stress-strain curve clarifies the three main stages of metal deformation, which the specimen passes through before passing in fracture mode. First stage elastic deformation and the material in this stage is in reversible phase, while the second stage is uniform plastic deformation irreversible phase and third stage nonuniform plastic deformation irreversible phase.





(b)

Fig. 13. The failure mode of coupon model under tensile test on (a) the numerical [11] and (b) numerical model of current study

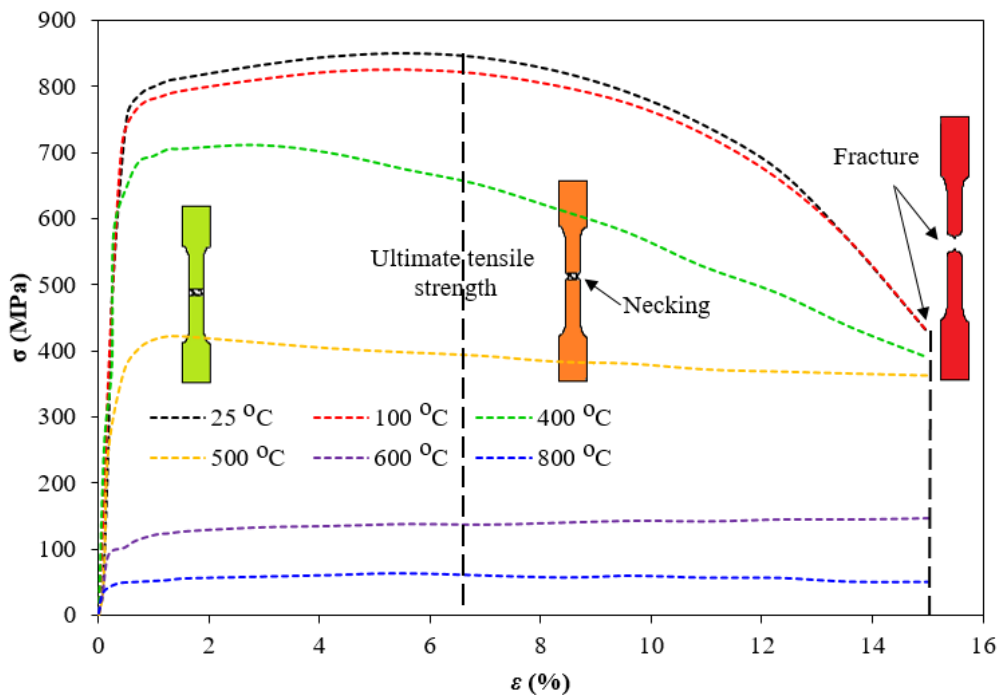


Fig. 14. The stress-strain curve at various temperature

4. Conclusion

The present study was designed to determine the effect of TIG welding on the thermo-mechanical performance of AISI 304 butt joints. The aim can be achieved by employing three-dimensional analysis with non-linear thermo-mechanical simulations for AISI 304 stainless steel using finite element analysis. This study has shown that when the welding current increases, the heat input increased and the fusion zone area is decreased. Increasing welding current (increase the heat input) leads to a reduction in cooling rate and an increasing the grain size of weld metal and heat affected zone. An increase welding current lead to increases the width of heat-affected zone and increases the volume fraction and decreases the microhardness. The results showed that the longitudinal

residual stress distribution is uniform along the weld line with similar pattern with transversal residual stress. However, at the starting and ending region of the weld line, the longitudinal and transversal residual stress have a compressive nature and its magnitude higher than longitudinal residual stress. Therefore, due to increase cooling rate, the microhardness has a maximum value at the boundary between the fusion zone and heat-affected zone. Nevertheless, the finite element model displayed that the coupon of AISI 304 was failed at the heat-affected zone region by necking and fracture heat-affected zone. Nevertheless, it turned out that all coupons tested for butt joints fractured in the heat-affected zone (HAZ).

Acknowledgements

The authors would like to thank Tikrit University for providing laboratory facilities and financial support.

References

- [1] Amstead, Billy Howard, Myron L. Begeman, and Philip F. Ostwald. *Manufacturing processes*. Wiley, 1987.
- [2] Zhang, Chaohua, Suo Li, Long Hu, and Dean Deng. "Effects of pass arrangement on angular distortion, residual stresses and lamellar tearing tendency in thick-plate T-joints of low alloy steel." *Journal of Materials Processing Technology* 274 (2019): 116293.
- [3] Bhadra, Rakesh, Pardeep Pankaj, Pankaj Biswas, and U. S. Dixit. "Thermo-mechanical analysis of CO₂ laser butt welding on AISI 304 steel thin plates." *International Journal of Steel Structures* 19, no. 1 (2019): 14-27.
- [4] Tashiro, Shinichi, Manabu Tanaka, and Masao Ushio. "Numerical simulation of gas tungsten arc welding in different gaseous atmospheres." *Transactions of JWRI* 34, no. 2 (2005): 1-5.
- [5] Cosson, Benoît, André Chateau, Akué Asséko, Mylène Lagardère, and Myriam Dauphin. "3D modeling of thermoplastic composites laser welding process—A ray tracing method coupled with finite element method." *Optics & Laser Technology* 119 (2019): 105585.
- [6] Sun, Yao, Yating Liang, and Ou Zhao. "Testing, numerical modelling and design of S690 high strength steel welded I-section stub columns." *Journal of Constructional Steel Research* 159 (2019): 521-533.
- [7] Hsu, Y. F., and B. Rubinsky. "Two-dimensional heat transfer study on the keyhole plasma arc welding process." *International Journal of Heat and Mass Transfer* 31, no. 7 (1988): 1409-1421.
- [8] Francis, Justin David. "Welding simulations of aluminum alloy joints by finite element analysis." PhD diss., Virginia Tech, 2001.
- [9] Martinussen, Mads. "Numerical modelling and model reduction of heat flow in robotic welding." Master's thesis, Institutt for teknisk kybernetikk, 2007.
- [10] Jiang, Wenchun, X. P. Xu, J. M. Gong, and S. T. Tu. "Influence of repair length on residual stress in the repair weld of a clad plate." *Nuclear Engineering and Design* 246 (2012): 211-219.
- [11] Chen, Cheng, Sing-Ping Chiew, Ming-Shan Zhao, Chi-King Lee, and Tat-Ching Fung. "Welding effect on tensile strength of grade S690Q steel butt joint." *Journal of Constructional Steel Research* 153 (2019): 153-168.
- [12] Borrmann, S., C. Kratzsch, L. Halbauer, A. Buchwalder, H. Biermann, I. Saenko, K. Chattopadhyay, and R. Schwarze. "Electron beam welding of CrMnNi-steels: CFD-modeling with temperature sensitive thermophysical properties." *International Journal of Heat and Mass Transfer* 139 (2019): 442-455.
- [13] Ficquet, Xavier. "Development and application of the deep hole drilling method." PhD diss., University of Bristol, 2007.
- [14] 乔羚. "Effect of geometric shape of plate on residual stress and deformation distribution for butt-weld joint." *中国焊接* 27, no. 3 (2018): 0.
- [15] Coules, H. E., D. J. Smith, K. Abburi Venkata, and C. E. Truman. "A method for reconstruction of residual stress fields from measurements made in an incompatible region." *International Journal of Solids and Structures* 51, no. 10 (2014): 1980-1990.
- [16] Bao, Rui, Xiang Zhang, and Norvahida Ahmad Yahaya. "Evaluating stress intensity factors due to weld residual stresses by the weight function and finite element methods." *Engineering Fracture Mechanics* 77, no. 13 (2010): 2550-2566.
- [17] Wang Xijing, W.B., Zhang Liangliang, Liu Xiao, and Yang Chao. "Mechanical properties and microstructure of pure nickel PAW and PAW-TIG welded joints." *China Welding* 26, no. 4 (2017): 37-47.
- [18] ANSYS, *ANSYS FLUENT V15 Theory Guide*. ANSYS Inc., USA, 2015.

- [19] Falkowicz, Katarzyna, Hubert Dębski, Paweł Wysmulski, and Patryk Różyło. "The behaviour of compressed plate with a central cut-out, made of composite in an asymmetrical arrangement of layers." *Composite Structures* 214 (2019): 406-413.
- [20] Alkumait, Aadel Abdul Razzaq, Maki Haj Zaidan, and Thamir Khalil Ibrahim. "Numerical Investigation of Forced Convection Flow over Backward Facing Step Affected By A Baffle Position." *Journal of Advanced Research in Fluid Mechanics and Thermal Sciences* 52, no. 1 (2018): 33-45.
- [21] Vakili-Tahami, Farid, and Ali Ziaei-Asl. "Numerical and experimental investigation of T-shape fillet welding of AISI 304 stainless steel plates." *Materials & design* 47 (2013): 615-623.
- [22] Pirinen, Markku, Yu Martikainen, P. D. Layus, V. A. Karkhin, and S. Yu Ivanov. "Effect of heat input on the mechanical properties of welded joints in high-strength steels." *Welding International* 30, no. 2 (2016): 129-132.
- [23] Choi, J., and Jyoti Mazumder. "Numerical and experimental analysis for solidification and residual stress in the GMAW process for AISI 304 stainless steel." *Journal of Materials Science* 37, no. 10 (2002): 2143-2158.
- [24] Jiang, W. C., B. Y. Wang, J. M. Gong, and S. T. Tu. "Finite element analysis of the effect of welding heat input and layer number on residual stress in repair welds for a stainless steel clad plate." *Materials & Design* 32, no. 5 (2011): 2851-2857.